JOURNAL OF Materials CHEMISTRY

Hydrothermal assembly and crystal structures of three novel open frameworks based on molybdenum(VI) oxides

Yan Xu,* Jianjiang Lu and Ngoh K. Goh

School of Science, Nanyang Technological University, Singapore 259756, Republic of Singapore. E-mail: yxu@nie.edu.sg

Received 1st March 1999, Accepted 26th April 1999

The hydrothermal syntheses, crystal structures and thermal behaviours of three new 3-D framework molybdenum(VI) oxide hybrid materials, $[MoO_3(pyz)_{0.5}]$ **1** (pyz = pyrazine), $[\{Cu(pip)_{0.5}\}MoO_4]$ (pip = piperazine) **2** and $[H_2Mo_2Cu_3O_{10}]$ **3**, are presented. **1** and **2** that are hybrids of inorganic oxide layers and bridging organodiamine ligands exhibit a covalent/coordination framework connectivity. **3** represents a novel open framework example of bimetallic oxides based on Mo^{VI} and Cu^{II}. These new materials are synthesized by a judicious selection of organodiamines accompanied by the concurrent alteration of initial reaction conditions. The choice of organodiamines is found to be critical to the framework composition and construction of solid architectures. The chiral framework of **1** and the 3-D structure of **2** are characterised by one-dimensional channels along the orthorhombic and triclinic *b* axis respectively circumscribed by six $\{MoO_5N\}$ octahedra and two pyz molecules in **1,** and by two $\{MoO_4\}$ tetrahedra, four $\{CuO_4N\}$ square pyramids and two pip molecules in **2**. The 3-D open framework of **3** has six-ring channels along the triclinic *b* axis. The thermal behaviours of the three solids are similar, undergoing a phase transition in the range 260–420 °C upon the removal of organic ligands in **1** and **2** and dehydration in **3**.

Introduction

A great deal of contemporary effort has been devoted to the development of rational synthetic routes to low-dimensional and porous crystalline materials for their possible applications in catalysis, separations, magnetism and optics. The achievement in this light is evident as demonstrated by the discovery of diamondoid networks[1–3] and the crystal engineering of novel solid architectures including octahedral,[4] honey comb,[5,6] square grid,[7,8] brick wall,[9] ladder,[10] and railroad motifs.[11] A significant part of this research is concerned with the construction of organic scaffolding, usually *N,N′*-donor bidentate ligands, through inorganic tethers such as Cu^{I}, Ag^{I}, Cu^{II}, Zn^{II} and Cd^{II}.[12] A strategy that is largely exercised in the design of these novel solid architectures is a 'modular construction concept'.[3] Recent observations reveal that this strategy can be extrapolated to the construction of inorganic covalent skeletons through the linkages of organic tethering units by forming coordination bonds. Successful examples include the syntheses of a number of novel low-dimensional and porous metal oxides/organic interwoven nets.[13]

Crystal engineering of metal oxides/organic coordination polymers can be achieved by linking inorganic components through *N,N′*-donor polydentate ligands.[13*b–d*] In the course of our investigation of the crystal engineering of molybendum(VI) oxide hybrid materials, we have produced a series of low-dimensional solids built up from inorganic clusters linked through transition metal–ethylenediamine complex groups.[14] Inspired by the recent success in the self-assembly of novel Mo–Cu oxide hybrid materials using various types of organoamine ligands,[13*c*] we set out to study the crystal engineering of Mo–Cu oxides in the presence of aromatic diamine, pyrazine (pyz), and aliphatic diamines, piperazine (pip) and 1,4-diazabicyclo[2.2.2]octane (DABCO), of various sizes. We report here the hydrothermal assembly and crystal structures of three novel open frameworks based on molybdenum(VI) oxides, $[MoO_3(pyz)_{0.5}]$ **1**, $[\{Cu(pip)_{0.5}\}MoO_4]$ **2** and $[H_2Mo_2Cu_3O_{10}]$ **3**. The 3-D architectures of **1** and **2** are constructed from the two-dimensional metal oxide layers and interweaving diamines, pyz and pip, where nitrogen donors coordinate to the metal centers of adjacent layers. Solid **3** is a bimetallic oxide having porous framework structure. Solid **1** is the first 3-D chiral framework molybdenum oxide hybrid material assembled by direct linking of Mo^{VI} octahedral centers through pyz bidentate ligands. The outstanding feature of solids **2** and **3** lies in the tetrahedral coordination geometry of Mo^{VI}.

Experimental

Synthesis

Preparations were exclusively carried out under hydrothermal autogenous pressure conditions in polytetrafluoroethylene (PTFE)-lined stainless steel autoclave reactors (≈22 ml). Starting materials included $MoO_3 \cdot H_2O$ (Ajax), pyz (Aldrich), pip (Aldrich), DABCO (Merck) and distilled H_2O (Lab-made). All reagents were used as received without further purification. No hazards were encountered during the experimental work. All crystalline products were recovered by filtration and repeated washing with distilled H_2O.

$[MoO_3(pyz)_{0.5}]$ **1** was prepared from the hydrothermal reaction of MoO_3 (0.16 g), $CuCl_2 \cdot 2H_2O$ (0.11 g), pyz (0.23 g) and H_2O (20 g) in the mole ratio of 1.5 : 1 : 4.5 : 1722 at 160 °C for 72 h. Light-coloured thin plates of **1** were recovered in 60% yield. $[\{Cu(pip)_{0.5}\}MoO_4]$ **2** was obtained in 85% yield from the hydrothermal reaction of MoO_3 (0.27 g), $CuCl_2 \cdot 2H_2O$ (0.23 g), pip (0.15 g) and H_2O (20 g) in the mole ratio of 1.3 : 1 : 1.3 : 823 at 160 °C for 72 h. The blue crystals of **2** were consistent with the Cu^{II} oxidation state. A sharp and strong IR band at 3166 cm^{-1} was in accord with the presence of the non-hydrogen bonded N–H group of pip. $[H_2Mo_2Cu_3O_{10}]$ **3** was isolated in 90% yield from the hydrothermal reaction of MoO_3 (0.46 g), $CuCl_2 \cdot 2H_2O$ (0.35 g), DABCO (0.42 g) and H_2O (20 g) in the mole ratio of 1.4 : 1 : 1.8 : 542 after 72 h at 160 °C. Light blue crystals of **3** were indicative of the Cu^{II} oxidation state. A strong IR band at 3440 cm^{-1} was in line with the presence of terminal OH groups.

Characterisation

Single crystal X-ray diffraction structure analysis. Crystal structures of **1–3** were determined from single crystal X-ray

Table 1 Crystal data and refinement details for **1–3**

	1	**2**	**3**
Formula	$CHMo_{0.5}N_{0.5}O_{1.5}$	$C_2H_5CuMoNO_4$	$HCu_{1.5}MoO_5$
M	91.99	266.55	272.26
Crystal system	Orthorhombic	Triclinic	Triclinic
Space group	$I222$	$P\bar{1}$	$P\bar{1}$
a/Å	5.270(2)	5.568(2)	5.358(6)
b/Å	5.2674(7)	6.829(2)	5.57(2)
c/Å	14.2310(11)	9.2460(12)	7.632(6)
α/°		100.716(12)	103.7(2)
β/°		101.52(2)	106.25(9)
γ/°		112.50(3)	97.4(2)
V/Å^3	395.06(13)	304.56(13)	207.8(6)
Z	8	2	2
μ(Mo-Kα)/mm^{-1}	3.181	5.487	10.521
T/K	297	297	297
Absorption correction: T_{min}, T_{max}	0.8009, 0.9911	0.7592, 0.9923	0.7616, 0.9218
No. independent reflection, (R_{int})	375 (0.0159)	1379 (0.0158)	733 (0.0250)
No. variables	35	82	71
R_1 [$I>2\sigma(I)$]	0.0169	0.0254	0.0250
wR_2 [$I>2\sigma(I)$]	0.0414	0.0532	0.0645
S (goodness of fit)	1.194	1.067	1.067

diffraction data collected by θ–2θ scans on a Siemens P4 X-ray diffractometer with graphite-monochromated Mo-Kα radiation. Non-hydrogen atoms were refined anisotropically except for disordered atoms. The position of the hydrogen atom attached to a terminal oxo group in **3** was found from difference maps and those attached to carbon and nitrogen atoms of organic molecules were placed at calculated positions. A summary of crystal data and refinement details for **1**–**3** is shown in Table 1. Selected bond lengths and angles are given in Table 2.

CCDC reference number 1145/156. See http://www.rsc.org/suppdata/jm/1999/1599/, for crystallographic files in .cif format.

Simultaneous TGA/DTA. Simultaneous TGA/DTA was performed from RT to 800 °C in an N_2 stream at a flow rate of 10 °C min^{-1} on a SETARAM Labsys™ TG-DTA system. **1** exhibited a two-step weight loss of *ca.* 25% in the temperature range 320–370 °C, corresponding to the loss of pyz (calc. wt% = 22) followed by a non-reconstructive phase transition. **2** showed a broad weight loss of 26.5% in the temperature range 260–620 °C which was attributed to the loss of pip

Table 2 Selected bond lengths (Å) and angles (°) for **1**–**3**

1	Mo1–O1	1.681(3)	O1–Mo1–N1	180
	Mo1–O2	1.923(3)	O2–Mo1–O2#1[a]	161.0(3)
	Mo1–O2#1[a]	1.923(3)	O2#2[a]–Mo1–O2#3[a]	160.1(3)
	Mo1–O2#2[a]	1.929(3)	O2#1[a]–Mo1–O2#3[a]	88.35(3)
	Mo1–O2#3[a]	1.929(3)	O2–Mo1–O2#3[a]	88.38(3)
	Mo1–N1	2.483(3)	O2–Mo1–O2#2[a]	88.35(3)
			O2#1[a]–Mo1–O2#2[a]	88.38(3)
2	Mo1–O1	1.717(3)	O1–Mo1–O2	107.5(2)
	Mo1–O2	1.724(3)	O1–Mo1–O3	107.54(14)
	Mo1–O3	1.796(3)	O1–Mo1–O4	103.71(13)
	Mo1–O4	1.842(3)	O2–Mo1–O3	111.06(14)
	Cu1–O3#1[b]	1.944(3)	O3–Mo1–O4	113.14(13)
	Cu1–O4	1.967(2)	O2–Mo1–O4	113.33(14)
	Cu1–O4#2[b]	1.993(3)	O4–Cu1–N1	169.22(13)
	Cu1–N1	1.992(3)	O3#1[b]–Cu1–O4#2[b]	161.78(12)
	Cu1–O2#3[b]	2.190(3)	O2#3[b]–Cu1–N1	92.19(14)
			O2#3[b]–Cu1–O4#2[b]	91.24(12)
			O2#3[b]–Cu1–O3#1[b]	105.05(13)
			O2#3[b]–Cu1–O4	97.51(12)
3	Mo1–O4	1.745(7)	O4–Mo1–O1	111.1(2)
	Mo1–O1	1.748(4)	O4–Mo1–O3	109.2(3)
	Mo1–O3	1.767(6)	O4–Mo1–O2	108.6(2)
	Mo1–O2	1.791(4)	O1–Mo1–O2	108.9(2)
	Cu1–O3#1[c]	1.941(5)	O2–Mo1–O3	108.7(2)
	Cu1–O1#2[c]	1.960(5)	O1–Mo1–O3	110.4(2)
	Cu1–O5	1.992(5)	O4–Cu1–O2#4[c]	176.29(14)
	Cu1–O5#3[c]	1.998(6)	O3#1[c]–Cu1–O1#2[c]	96.3(2)
	Cu1–O4	2.287(7)	O3#1[c]–Cu1–O5#3[c]	91.0(3)
	Cu1–O2#4[c]	2.412(8)	O5–Cu1–O5#3[c]	80.9(2)
	Cu2–O2#5[c]	1.941(5)	O1#2[c]–Cu1–O5	94.3(2)
	Cu2–O2#6[c]	1.941(5)	O5–Cu2–O2#6[c]	94.0(2)
	Cu2–O5	1.987(6)	O5–Cu2–O2#5[c]	86.0(2)
	Cu2–O5#7[c]	1.987(6)	O4–Cu2–O5	81.6(2)
	Cu2–O4	2.463(7)	O4–Cu2–O2#5[c]	92.1(2)
	Cu2–O4	2.463(7)	O4–Cu2–O2#6[c]	93.3(2)

Symmetry transformations used to generate equivalent atoms: [a]#1 $-x+1$, $-y+1$, z; #2 $-x+3/2$, $y-1/2$, $-z+3/2$; #3 $x-1/2$, $-y+3/2$, $-z+3/2$. [b]#1 $-x+1$, $-y+1$, $-z+1$; #2 $-x+1$, $-y+2$, $-z+1$; #3 $x-1$, y, z. [c]#1 x, $y+1$, z; #2 $-x+1$, $-y+1$, $-z+1$; #3 $-x+2$, $-y+2$, $-z+2$; #4 $x+1$, $y+1$, z; #5 $-x+1$, $-y+1$, $-z+2$; #6 $x+1$, y, z; #7 $-x+2$, $-y+1$, $-z+2$.

(calc. wt% = 16, 260–340 °C) followed by a reconstructive phase transition (340–620 °C). **3** showed a sharp weight loss of *ca.* 3% in the range 370–420 °C due to dehydration between terminal OH groups (calc. wt% = 3.1) accompanied by a phase transition.

Powder X-ray diffraction and infrared studies. XRD patterns were collected using a Siemens D5005 diffractometer with graphite-monochromated Cu-Kα radiation ($\lambda = 1.5418$ Å) in the range $3.5 < 2\theta < 60°$. IR spectra (KBr pellet) were recorded on a Perkin-Elmer FT-IR spectrometer in the range 4000 to 450 cm^{-1}.

Results and discussion

$[MoO_3(pyz)_{0.5}]$ **1** crystallises from a hydrothermal mixture composed of MoO_3, $CuCl_2{\cdot}2H_2O$, pyz and H_2O. The presence of $CuCl_2{\cdot}2H_2O$ is found to be critical for the successful synthesis of **1**; the use of $CuSO_4{\cdot}5H_2O$ instead fails to give the same crystalline phase. Modification of the metal oxide backbone is accomplished in a reaction system containing an aliphatic diamine, pip. The hydrothermal reaction of MoO_3, $CuCl_2{\cdot}2H_2O$, pip and H_2O produces monophasic crystals of $[\{Cu(pip)_{0.5}\}MoO_4]$ **2**. The successful incorporation of Cu^{II} into the inorganic matrix is associated with the replacement of pyz with pip, and a more quantitative evaluation of its cause is being made.

$[\{Cu(pip)_{0.5}\}MoO_4]$ **2** is the third member of the 3-D interwoven $[Cu\{diamine\}_nMoO_4]$ family, the other two being $[\{Cu(dpe)\}MoO_4]$[13b] [dpe = 1,2-*trans*-(4-pyridyl)ethane] and $[\{Cu(bpa)_{0.5}\}MoO_4]$,[13c] (bpa = bipyridylamine) built up of $[MoCuO_4]$ inorganic layers and diamine ligands. It is remarkable to see the range of structural versatility of the same inorganic stoichiometry of $[MoCuO_4]$ evolved from the introduction of different diamine donors. Extrapolating this rationale to a hydrothermal reaction system containing a large aliphatic diamine, DABCO, a novel 3-D open framework bimetallic oxide $[H_2Mo_2Cu_3O_{10}]$ **3** is isolated, in which DABCO is absent.

$[MoO_3(pyz)_{0.5}]$ **1** crystallises in a non-centrosymmetric space group *I*222. The structure of **1** consists of layers of corner-sharing $\{MoO_5N\}$ octahedra parallel to the *ab* plane linked through pyz molecules into a 3-D molybdenum oxide/pyz chiral framework (Fig. 1). The 3-D architecture of **1** can be described as an interwoven net of inorganic metal oxide layers (Fig. 1 inset) and organic tethers. The molybdenum oxide layers are stacked along the *c* axis in an ABAB… sequence. The connectivity between the molybdenum oxide layers and pyz molecules results in one-dimensional rectangular channels along the *b* axis circumscribed by six $\{MoO_5N\}$ octahedra and two pyz molecules. The coordination geometry at the Mo site is defined by one terminal oxo group, two pairs of bridging oxo groups and one pyz nitrogen dornor with the Mo–O bond lengths of 1.681(3), $2 \times 1.923(3)$, $2 \times 1.929(3)$ and the Mo–N length of 2.483(3) Å. This geometry deviates from the common 'two short–two intermediate–two long' bond length pattern of molybdenum oxides. The significant lengthening in the Mo–N distance reflects the strong *trans* effects of the terminal oxo group. The pyz carbon atom is distorted, hence the fourfold crystal symmetry of **1** is prevented.

The structure of **2** is constructed from $[MoCuO_4]$ layers parallel to the *ab* plane bridged through pip ligands into a 3-D covalent/coordination framework (Fig. 2). The metal oxide layer can be envisioned as being built up of $[MoCuO_4]$ chains of corner-sharing $\{MoO_4\}$ tetrahedra and $\{CuO_4N\}$ square pyramids in space group $P\bar{1}$ linked by corner-shared oxo groups between $\{MoO_4\}$ and $\{CuO_4N\}$ of adjacent chains (Fig. 2 inset). The fundamental motif of **2** consists of a regular tetrahedral Mo^{VI} center coordinated to three $\{CuO_4N\}$ square

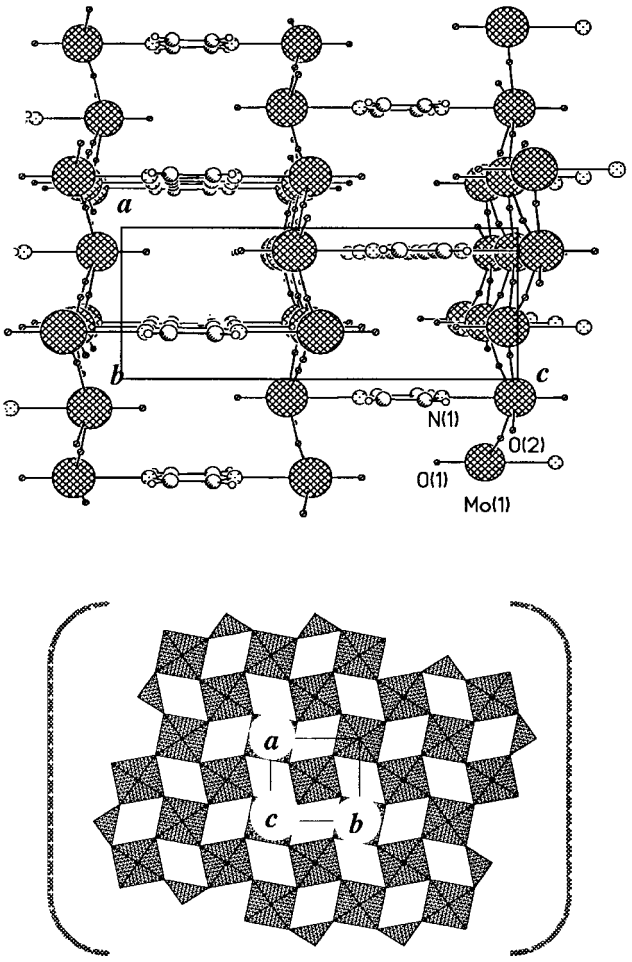

Fig. 1 Crystal structure of $[MoO_3(pyz)_{0.5}]$ **1** viewed along the *b* axis. Coordination of pyrazine ligands to molybdenum oxide layers results in a 3-D inorganic–organic framework with 1-D rectangular channels. (Inset) a projection of molybdenum oxide layers of **1** on the *ab* plane showing the polyhedral connectivity and four-membered rings circumscribed by four $\{MoO_6\}$ octahedra.

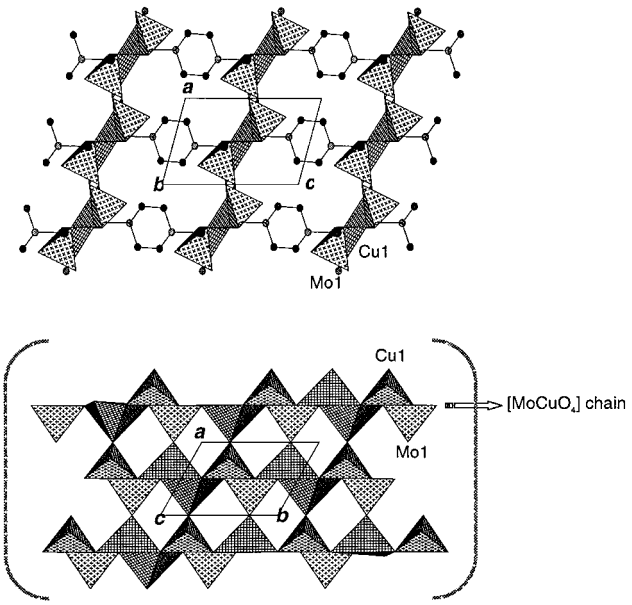

Fig. 2 A view of the structure of $[\{Cu(pip)_{0.5}\}MoO_4]$ **2** along the *b* axis showing 1-D channels and 3-D covalent/coordination framework constructed from $[MoCuO_4]$ layers linked through piperazine bridges. (Inset) a view down the *c* axis illustrating the $[MoCuO_4]$ layer structure of $[\{Cu(pip)_{0.5}\}MoO_4]$ **2**.

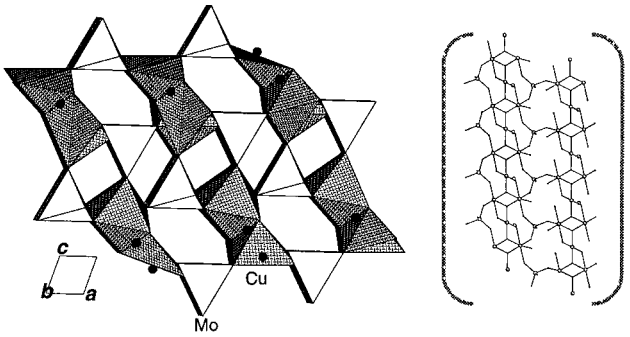

Fig. 3 A view of the structure of $[H_2Mo_2Cu_3O_{10}]$ **3** along the *b* axis highlights the four- and six-ring channels. (Inset) connectivity between $\{Cu_3\}$ chains of **3** linked through $\{MoO_4\}$ tetrahedra.

pyramids, each containing a half pip molecule. The molybdenum site possesses one terminal oxo group pointing nearly perpendicular to the plane. The square pyramidal geometry at the Cu site together with the blue colour of **2** indicate the Cu^{II} oxidation state. The equatorial positions of $\{CuO_4N\}$ are occupied by three oxo groups and one pip N donor and the axial position by one oxo group linking to a $\{MoO_4\}$ tetrahedron of the neighbouring chain. The adjacent $[MoCuO_4]$ layers are connected through pip ligands that are oriented at an angle of *ca.* 74° to the least-squares plane of the inorganic layers giving rise to the 3-D bimetallic oxide/diamine solid architecture. This coordination connectivity generates one-dimensional parallelogram-shaped channels along the *b* axis circumscribed by two $\{MoO_4\}$ tetrahedra, four $\{CuO_4N\}$ square pyramids and two pip molecules.

The structure of **3** consists of a 3-D framework of $\{MoO_4\}$ tetrahedra and $\{CuO_6\}$ octahedra connected *via* shared corners between $\{MoO_4\}$ and $\{CuO_6\}$, and shared edges between $\{CuO_6\}$ octahedra (Fig. 3). It can be conceptually viewed as being built up in space group $P\bar{1}$ from chains of $\{Cu_3\}$ trimers bridged through $\{MoO_4\}$ tetrahedra into a 3-D covalent framework. The $\{Cu_3\}$ chain, which is parallel to the *b* axis, can be described as a spiral of two 2-rings packed through a center of symmetry at one of the copper atoms. The polyhedral connectivity between the $\{Cu_3\}$ chains and $\{MoO_4\}$ units gives rise to intersecting 4-ring straight channels of $(MoCu_3)$ and (Mo_2Cu_2) along the *a* and *b* axes respectively and one-dimensional 6-ring straight channels of (Mo_2Cu_4) along the *b* axis. The negative charges of the $[Mo_2Cu_3O_{10}]^{2-}$ framework are compensated by protons, which are readily located from Fourier maps, attached to one of the two $\{CuO_6\}$ octahedra. The geometric configurations of the $\{MoO_4\}$ tetrahedron and $\{CuO_6\}$ octahedra are as expected while Jahn–Teller distortions are observed at both Cu sites (axial Cu–O 2.287(7), 2.412(8) Å at Cu1, $2 \times 2.463(7)$ Å at Cu2). The assignment of the +2 oxidation state of Cu is supported by their octahedral geometries and the colour of the crystals of **3**.

The absence of a DABCO molecule from the structure of **3** might be in part due to its large dimensions and in part due to the poor match between the charge density of the inorganic and organic components. The synthesis of **3** reveals the critical control of the matching charge density between the counter ions on the successful construction of 3-D architectures. It also offers promises for the future investigation of the crystal engineering of 3-D MoMO frameworks with yet larger pores by the use of bigger cations of either organic or inorganic nature.

The successful syntheses of 3-D solids **1–3** illustrate the structural versatility of molybdenum oxides evolving from the introduction of appropriate *N,N′*-bidentate components acting as structural tethers and the use of heteroatoms, *e.g.* transition metal ions. It is evident that the close matching in the charge density between modular components plays a critical role in forming 3-D covalent/coordination polymers, though the mechanism by which the self-assembly process is organised remains elusive. The roles that heteroatoms play are twofold: (i) providing linkages and (ii) altering the charge density of the inorganic matrix. The present compounds suggest that a vast family of open framework molybdenum oxide hybrid materials may be assembled by appropriate use of organic or inorganic bridging groups coupled with judicious adjustment of reaction pH, solvents and the use of mineralisers. It appears that this rationale of crystal engineering provides a facile method for structural modification of inorganic composite materials and, consequently, tuning of their chemical and physical properties.

Acknowledgements

We would like to thank Nanyang Technological University for financial support (RP 17/97 XY). We are grateful to the technical staff in the Division of Chemistry, School of Science for support services.

References

1 M. J. Zaworotko, *Chem. Soc. Rev.*, 1994, 283 and refs. therein.
2 O. M. Yaghi and H. Li, *J. Am. Chem. Soc.*, 1995, **117**, 10401.
3 B. F. Hoskins and R. Robson, *J. Am. Chem. Soc.*, 1990, **112**, 1546 and refs. therein.
4 S. Subramanian and M. J. Zaworotko, *Angew. Chem.*, *Int. Ed. Engl.*, 1995, **34**, 2127.
5 L. R. MacGillivray, S. Subramamian and M. J. Zaworotko, *J. Chem. Soc.*, *Chem. Commun.*, 1994, 1325.
6 G. B. Gardner, D. Venkataran, J. S. Moore and S. Lee, *Nature* (*London*), 1995, **374**, 792.
7 R. W. Gable, B. F. Hoskins and R. Robson, *J. Chem. Soc.*, *Chem. Commun.*, 1990, 1677.
8 M. Fujita, Y. J. Kwon, S. Washizu and K. Ogure, *J. Am. Chem. Soc.*, 1994, **116**, 1151.
9 M. Fujita, Y. J. Kwon, O. Sasaki, K. Yamaguchi and K. Oguna, *J. Am. Chem. Soc.*, 1995, **117**, 7287.
10 P. Losier and M. J. Zaworotko, *Angew. Chem.*, *Int. Ed. Engl.*, 1996, **35**, 2779.
11 O. M. Yaghi, H. Li and T. L. Groy, *Inorg. Chem.*, 1997, **36**, 4292.
12 A. J. Blake, N. R. Champness, S. S. M. Chung, W. Li and M. Schröder, *Chem. Commun.*, 1997, 1005.
13 (*a*) D. Hagrman, C. Zubieta, D. J. Rose, J. Zubieta and R. C. Haushalter, *Angew. Chem.*, *Int. Ed. Engl.*, 1997, **36**, 873; (*b*) D. Hagrman, R. C. Haushalter and J. Zubieta, *Chem. Mater.*, 1998, **10**, 361; (*c*) D. Hagrman, C. J. Warren, R. C. Haushalter, C. Seip, C. J. O'Connor, R. S. Rarig, Jr., K. M. Johnson, III, R. L. LaDuca, Jr. and J. Zubieta, *Chem. Mater.*, 1998, **10**, 3294; (*d*) D. Hagrman, P. J. Zapf and J. Zubieta, *Chem. Commun.*, 1998, 1283.
14 J. J. Lu, Y. Xu, N. K. Goh and L. S. Chia, *Chem. Commun.*, 1998, 2733.

Paper 9/01592B